A Matrix-Inversion-Free Fixed-Point Method for Distributed Power Flow Analysis

Kishan Prudhvi Guddanti [ID], *Student Member, IEEE*, Yang Weng [ID], *Senior Member, IEEE*, and Baosen Zhang [ID], *Member, IEEE*

Abstract—The power flow (PF) problem is a fundamental problem in power system engineering. Many popular solvers like PF and optimal PF (OPF) face challenges, such as divergence and network information sharing between multi-areas. One can try to rewrite the PF problem into a fixed point (FP) equation (more stable), which can be solved exponentially fast. But, existing FP methods are not distributed and also have unrealistic assumptions such as requiring a specific network topology. While preserving its stable nature, a novel FP equation that is distributed in nature is proposed to calculate the voltage at each bus. This distributed computation enables the proposed algorithm to compute the voltages for multi-area networks without sharing private topology information. Unlike existing distributed methods, the proposed method does not use any approximate network equivalents to represent the neighboring area. Thus, it is approximation-free, and it also finds use cases in distributed AC OPFs. We compare the performance of our FP algorithm with state-of-the-art methods, showing that the proposed method can correctly find the solutions when other methods cannot, due to high condition number matrices. In addition, we empirically show that the FP algorithm is more robust to bad initialization points than the existing methods.

Index Terms—Distributed power flow, fixed-point equation, multi-area network power flow, ill-conditioned problems.

NOMENCLATURE

Bold signifies a vector.

(a_p, b_p, c_p)	Three tuple describing the circle representing the real power equation.
(a_q, b_q, c_q)	Three tuple describing the circle representing the reactive power equation.
$\mathbf{1}$	Vector of 1's of appropriate length.
$\Delta \mathbb{S}$	Apparent power mismatch of a bus with the largest mismatch in the entire power network.
ΔV	Vector of change in voltage state at all buses in the network.

$\mathbf{B}$	Vector with bus type information of all buses in the network.
$\mathbf{b}_d$	Vector of susceptances of all branches connecting bus d and its neighbors $\mathcal{N}(d)$.
$\mathbf{g}_d$	Vector of conductances of all branches connecting bus d and its neighbors $\mathcal{N}(d)$.
$\mathbf{o}_p, \mathbf{o}_q$	Centers of the circles representing real and reactive power equations respectively.
$\mathbf{u}$	Vector with concatenation of all real ($v_{k,r} \ \forall k \in \mathcal{N}(d)$) followed by all imaginary ($v_{k,i} \ \forall k \in \mathcal{N}(d)$) voltage parts of the neighboring buses to bus d.
$\mathbf{v}$	Vector of complex voltages at all buses in the power network.
$\boldsymbol{\Delta} S$	Vector of difference between the actual and calculated apparent powers at all buses in the network.
λ	Load (real, reactive powers) and generation (real power) scaling factor.
$\mathcal{N}(d)$	Set of neighboring buses connected to bus d.
ζ	Tolerance for the convergence of the algorithm.
$C^{\perp}$	Orthogonal circle that passes through the intersections of the real and reactive power circles.
$g_{d,k}, \ b_{d,k}$	Conductance and susceptance of the branch connecting buses d and k.
J	Jacobian matrix.
$p_d, \ q_d$	Net real and reactive power injections at bus d.
$P_i, \ Q_i$	Specified net real and reactive power injections at bus i.
$Q_{max}, \ Q_{min}$	Upper and lower reactive power limits of a PV bus.
$r_p, \ r_q$	Radii of the circles representing real and reactive power equations respectively.
$v_{d,r}, \ v_{d,i}$	Real and imaginary parts of the complex voltage (v_d) at bus d.
V_{ref}	Specified voltage magnitude of a PV bus.

I. INTRODUCTION

THE power flow problem is one of the canonical problems in power engineering and it is frequently used in power system operation and planning studies [1]. Existing power flow methods mostly rely on iterative methods such as Newton-Raphson (NR) [2] or fast decoupled load flow (FDLF) [3], [4]. These algorithms have been the workhorses of the power

industry and have performed well most of the time. Additionally, due to the popularity of electric and autonomous vehicles, the state power grids are seeing an alarming demand growth, and some utilities have even issued statements about overloaded circuits [5]–[7]. Furthermore, this demand growth is also coupled with commercial and industrial developments. As large-scale development of renewable resources and distributed generation push systems to operate in new regimes, the existing algorithms can experience convergence issues, especially when systems operate close to their loadability limits [8]. Therefore, the need for new efficient and robust power flow algorithms to complement these existing methods remains despite decades of studies [9].

Algorithms like NR can be thought as variants of descent algorithms (or approximate descent in the case of FDLF) that modifies the solution iteratively. A fundamental reason for why these algorithms can fail to converge to a solution is simply because the geometry of power flow is not convex [10], [11]. For example, NR uses the Jacobian to find the direction of the steepest descent. Because the power flow equations are nonlinear and non-convex, there are many local minimums and saddle points, and the Jacobian-based power flow solvers fails to converge to a decent solution. This is because the gradient value becomes zero at these points and the Jacobian-based power flow solvers get stuck at these points. To prevent the algorithm from getting stuck, it becomes important to pick "good" initial starting points [12], [13]. Consequently, a number of methods have been developed to overcome the sensitive dependence on the initial guess [14], [15].

As systems start to operate closer to their limits, picking better initialization points becomes insufficient. Since the Jacobians for all points that are close to the boundary of the feasible power flow region have eigenvalues close to 0 (they loose rank), they necessarily become ill-conditioned and iterative algorithms may diverge [16], [17]. To avoid this phenomenon, a class of non-divergent power flow algorithms was developed to accelerate or decelerate the updates based on the conditioning of the Jacobian [18]–[21]. However, these approaches can still be sensitive to the initial guess and sometimes exhibit oscillatory behavior, where the solutions may neither converge nor diverge. An approach using complementarity conditions is developed in [22], but it can reach local minimums or saddle points instead of the true power flow solution. Energy-function analysis based on mechanical models can help algorithms to escape these stationary points [23], but implementing them for different bus types in a practical power system is non-trivial. Holomorphic embedding is used in [24], [25], but these algorithms are slower and require very high precision machines. Genetic algorithms such as [26] and [27] typically use Newton-Raphson (NR) as an inner loop, thus can struggle when the inner NR loop diverges. Robust NR power flow (e.g., [28] can prevent divergence, but may lead to algorithms that stall rather than converge to a true solution).

Recently, a new class of power flow formulations based on fixed point equations has been proposed mainly to overcome this ill-conditioning problem. This class of power flow solvers also overcome the algorithmic challenges present in descent algorithms [29], [30]. The basic idea is to write the power flow equations in a form of $\mathbf{v} = f(\mathbf{v})$, where $\mathbf{v}$ is the complex voltage and a fixed point of the function f [31]. If this relationship can be found, then a simple algorithm to find the fixed point is to repeatedly apply the function f. Furthermore, if the iterates converge to the fixed point, then it will converge exponentially quickly. The challenge is to find a suitable f, which have only exists for restricted class of systems. For example, the results in [30], [32] apply to networks with only PQ buses, and the result in [29] only applies to purely inductive (lossless) radial networks. Compared to the works in [33] and [34], they use matrix-based (i.e., needing to invert the Jacobian matrix), which experiences the same difficulty as more traditional power flow methods when the network becomes ill-conditioned. Therefore, there is a need for a fixed point function f that has no such limitations.

Hence, in this paper, we present a novel fixed point formulation of the full AC power flow equations that is applicable to networks with arbitrary topologies and mixture of PQ and PV buses. Additionally, with the restructuring of power sector, there is a need for localized algorithms between different areas of the system operated by different entities. This calls for distributed fixed point algorithms. Distributed methods like [35]–[37] use approximate network equivalents to represent the other area connected via a tie line but they are prone to inaccuracies. This work presents a distributed fixed point method that is also approximation-free and hence it is not prone to inaccuracies. This approach is based on a coordinate transformation, where power flow solutions are interpreted as the intersections of circles, where the parameters (center and radius) of the circles depend linearly on the voltages of the neighboring buses. This formulation can be thought as a generalization of the PV noise curve often used to visualize power transfer between two buses. Computationally, only the intersection of two circles needs to be calculated, which involves a series of simple algebraic computations. Therefore, this approach is much cheaper than other algorithms (e.g., NR) that require matrix calculations.

To verify the performance of our algorithm, we test it on the standard IEEE systems, including large ones with 2383 and 3375 buses. We compare our approach with NR, FDLF and non-divergent power flow algorithms. We show that when the loading is heavy, our algorithm is able to converge to the right solution while the other algorithm can diverge or become unstable. In addition, we show that our method is much more robust to random initialization points than the other methods. It is important to note that we are not advocating to replace existing power flow solvers. These algorithms have been highly optimized and do perform extremely well in many situations. Rather, the proposed algorithm in this paper can be used as a complementary tool by the system operators when conventional algorithm diverge or stall.

The paper is organized as follows: Section II introduces the rectangular power flow equations and show how they can be thought as intersections of circles. Section III discusses the fixed point formulation of the power flow equations and walks through a three-bus example. Section IV presents the main algorithm and its distributed feature with an example. Section IV-B introduces a 3-tuple vector form of circles and shows how closed-form
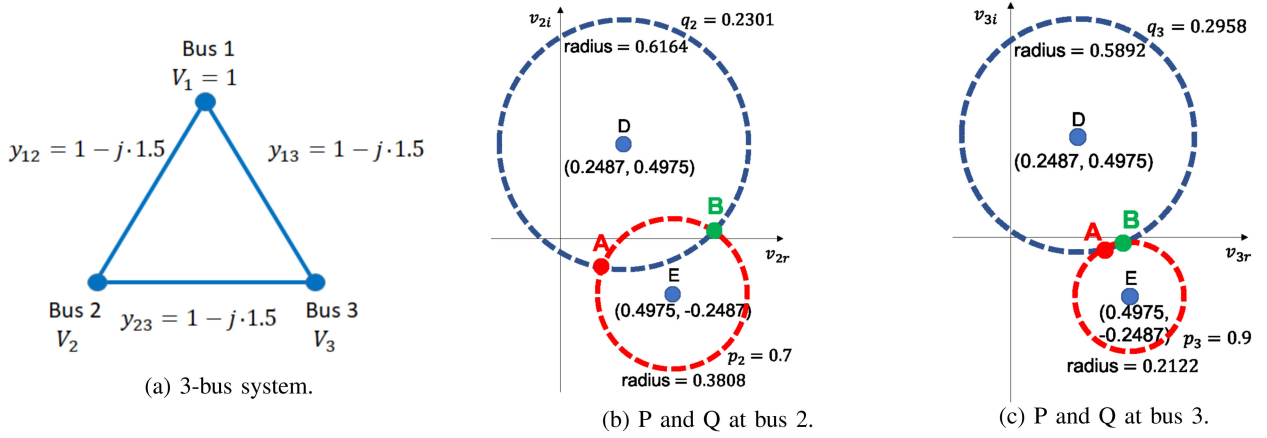
Fig. 1. Active and reactive circles for a three-bus system. Bus 1 is the slack bus and buses 2 and 3 are PQ buses.

formulas with good numerical properties can be found using the vector notation. Section V shows numerical results of our proposed algorithm compared against existing state-of-the-art algorithms on different IEEE benchmark networks. Section VI concludes the paper.

II. POWER FLOW EQUATIONS AND CIRCLES

A. Power Flow Equations in Rectangular Coordinates

To develop a distributed fixed point equation, first we have to formulate the traditional power flow equations at a bus in a distributed framework. This means that in order to solve for voltage at a bus, we must require only its neighboring bus information. This section presents this formulation using power flow circles.

Throughout this paper we use rectangular coordinates where a bus is index by d; p_d and q_d are the active and reactive powers, respectively; $v_{d,r}$ and $v_{d,i}$ are the real and imaginary parts of the bus voltage, respectively; and $\mathcal{N}(d)$ is the set of neighboring buses connected to bus d. We adopt the standard Π model of transmission lines and write the admittance of a line between buses d and k as $g_{dk} + jb_{dk}$. We assume that $b_{dk} \leq 0$ for all lines (lines are inductive). Shunt admittances and tap changing transformers are modeled with fixed tap ratios and incorporated into the admittance matrix using π equivalent representations.

In these notations, the power flow equations become:

$$p_d = t_{d,1} \cdot v_{d,r}^2 + t_{d,2} \cdot v_{d,r} + t_{d,1} \cdot v_{d,i}^2 + t_{d,3} \cdot v_{d,i}, \quad (1a)$$

$$q_d = t_{d,4} \cdot v_{d,r}^2 - t_{d,3} \cdot v_{d,r} + t_{d,4} \cdot v_{d,i}^2 + t_{d,2} \cdot v_{d,i}. \quad (1b)$$

The parameters $t_{d,1}, t_{d,2}, t_{d,3}, t_{d,4}$ are given by

$$t_{d,1} = - \sum_{k \in \mathcal{N}(d)} g_{k,d}, \ t_{d,2} = \sum_{k \in \mathcal{N}(d)} (v_{k,r} g_{k,d} - v_{k,i} b_{k,d}),$$

$$t_{d,3} = \sum_{k \in \mathcal{N}(d)} (v_{k,r} b_{k,d} + v_{k,i} g_{k,d}), \ t_{d,4} = \sum_{k \in \mathcal{N}(d)} b_{k,d}.$$

Since the terms $t_{d,1}$ and $t_{d,4}$ are always negative, (1a) and (1b) describe two circles in the variables $v_{d,r}$ and $v_{d,i}$. We call the

circle described by (1a) the active power circle parametrized by its center $\mathbf{o}_p$ and radius r_p; similarly, we say that (1b) describes the reactive power circle parameterized by center $\mathbf{o}_q$ and radius r_q. These parameters are given by:

$$\mathbf{o}_p = \left(\frac{-t_{d,2}}{2t_{d,1}}, \frac{-t_{d,3}}{2t_{d,1}} \right), \ \mathbf{o}_q = \left(\frac{t_{d,3}}{2t_{d,4}}, \frac{-t_{d,2}}{2t_{d,4}} \right), \quad (2a)$$

$$r_p = \sqrt{\frac{p_d}{t_{d,1}} + \frac{(t_{d,2})^2 + (t_{d,3})^2}{4t_{d,1}^2}}, \quad (2b)$$

$$r_q = \sqrt{\frac{q_d}{t_{d,4}} + \frac{(t_{d,3})^2 + (t_{d,2})^2}{4t_{d,4}^2}}. \quad (2c)$$

Fig. 1 shows a three bus network. The line admittance of all branches are $1 - j \cdot 1.5$. Bus 1 is considered to be a slack bus with a voltage of 1 p.u., while buses 2 and 3 are considered to be PQ buses. To demonstrate how the circles are drawn, assuming that we know the voltage phasor values at buses 1 and 3, using (2), as shown in Fig. 1(b), we can calculate the centers and radii for the power flow circles in (1) corresponding to bus 2. Similarly, we can also draw the power flow circles at bus 3 when the voltage phasor values at buses 1 and 2 known. The intersection points A and B in Fig. 1(b) represents the voltage phasor (power flow) solution at bus 2.

This voltage update computation at a bus is distributed in nature since (1) at bus d only requires its adjacent branch and neighboring buses voltage information. We will later show that when solving power flow problem using the proposed distributed iterative algorithm we can use estimates of the unknown neighboring bus voltage phasor values and we do not necessarily need to know the exact voltage phasor values of the neighboring bus voltages to calculate the power flow solution (voltage) at current bus.

B. PV Buses

The discussions in the above section focus on PQ buses, but PV buses are also frequently used to describe generators . In this case, the reactive power balance equation in (1b) is replaced by

a condition on the voltage magnitude:

$$v_{d,r}^2 + v_{d,i}^2 = V_{ref}^2, \tag{3}$$

where V_{ref} is the reference voltage. Again, we can think of PV buses in term of circles, since (3) is a circle centered at the origin with a fixed radius. Therefore, our framework does not require different treatment of PQ and PV buses.

III. Fixed Point Equation for Power Flow

The geometric representation of the power flow equations as the intersection of circles leads to a simple fixed point view of power flow solutions. Suppose that a vector of complex voltages is given. Then, the voltage at a particular bus d is determined by its neighbors alone (distributed) as the intersection of the active power circle with the reactive power circle (for a PQ bus) or with the voltage magnitude circle (for a PV bus). Of course, two circles, if they intersect, could do so at two distinct points as shown in Figs. 1(b) and 1(c). In this case, we need to pick one of the intersection points as the complex voltage at a bus and use it to compute the parameter of its neighboring circles. To make this choice, we follow two common assumptions made in power flow calculations.

The assumption we make is that we are interested in solutions at higher voltage magnitudes [38]. These solutions have long been seen as the practical and stable solutions in actual systems. For example, in both Figs. 1(b) and 1(c), we would chose point B as the solution. For a PV bus, all points of intersection have the same voltage magnitude. In this case, we make the second assumption that voltages with smaller (absolute) angles are preferable. This assumption is rooted in power system stability analysis, where smaller angles indicate more stable solutions [39].

With these choices, the complex voltage at a bus is uniquely determined by the complex voltages of its neighbors, which leads to a natural consistency condition for a solution. Given $\mathbf{v}$, let f be a function that takes $\mathbf{v}$ and performs the circle intersection operation (choosing a unique solution as described in the last paragraph). Then a vector $\mathbf{v}$ is a solution to the power flow problem if and only if $\mathbf{v} = f(\mathbf{v})$. That is, $\mathbf{v}$ is a fixed point of f. Note that if two circles do not intersect at a bus, then we can declare that $\mathbf{v}$ is not a fixed point.

Here, we use the three bus single area network in Fig. 1 to illustrate an algorithm to solve the power flow problem. The line admittance of all the branches are $1 - j \cdot 1.5$. Bus 1 is considered to be a slack bus with a voltage of 1 p.u., while buses 2 and 3 are considered to be PQ buses. Initially, the voltage $v_2 = v_{2,r} + jv_{2,i}$ at bus 2 is fixed with an initial guess. Based on v_2, the real and reactive power circles at bus 3 can be calculated. If these circles intersect with each other, the one with the higher voltage magnitude would be assigned as the value for v_3. Then, the voltage at bus 3 is fixed and intersections of the two circles at bus 2 are used to update v_2. This is repeated until the convergence is achieved. Next, we describe the algorithm for a general network.

IV. Main Algorithm

A. Description of the Distributed FP Algorithm

For an n-bus single area system, to start the algorithm, the voltages at all the buses in the system are fixed with an initial guess. Then the voltage solution at a bus is updated using its neighbors. This is repeated for all buses, which we call a round of the algorithm. The algorithm terminates if none of the buses update their complex power in a round or when the complex power mismatch is less than the tolerance set by the user. Algorithm 1 presents the pseudo code for a system with only PQ buses.

In the case of a multi-area system, as illustrated in Fig. 2, area 1 and area 2 contain the buses in red and green colors respectively. The boundary buses (buses 4 and 5) connect the two areas via a tie line. With the proposed approach, the power flow is solved for this multi-area power system in a distributed manner, in the sense that the red and green buses do not need to know the topology information about the other group. First, both area 1 and area 2 buses are initialized with a 1 p.u. voltage guess. Next, the voltage at each bus is calculated and simultaneously updated using the proposed fixed-point equation.

For example, as shown in Fig. 2, at iteration/round 1, bus 2 voltage is first calculated locally with the help of the proposed fixed-point equation that only requires the neighbors' (buses 1 and 4) voltages of bus 2. This calculated voltage phasor value is updated as bus $2'$ voltage simultaneously. This same approach is applied to bus 3 as well using its neighboring bus' (bus 4) voltage phasor value. To calculate the voltage at bus 4, its adjacent branch admittances and voltage values at buses $2,'$ $3,'$ and 5 are required. Using a communication between the two area operators, voltage iterate value at bus 5 (in this case at iteration 1, it is 1 p.u.) at the current iteration is shared with the area 1 operator to compute the voltage phasor iterate value at bus 4. This calculated voltage phasor value is updated as bus $4'$ voltage simultaneously. These similar steps are also carried out in area 2 to calculate and update the voltages at bus 5 (via communication) and at buses 6, 7 (locally). This total process (Algorithm 1) is repeated for several iterations/rounds until convergence. The highlight is that the two system operators does not need to share their area topology sensitive information with the other area since each voltage update at a bus in Algorithm 1 is a distributed computation.

Another important contribution is that unlike [35], [37], the proposed method does not use approximate network equivalents or decomposition techniques and hence, it is approximation-free and not prone to any inaccuracies. For a system with mixed PQ and PV buses, a similar algorithm is presented in Appendix. The exact distributed (18) to find the intersection will be explained in more details in Section IV-B. The exact order of updates is not constrained by the algorithm, although it is an interesting question to see if there exist an "optimal" update order in some sense.

It is possible that the circles do not intersect at a bus either at the start of the algorithm or during one of the iterations. In these cases, we simply restart the algorithm with a new initial guess. We note that for feasible problems with PQ buses, we have
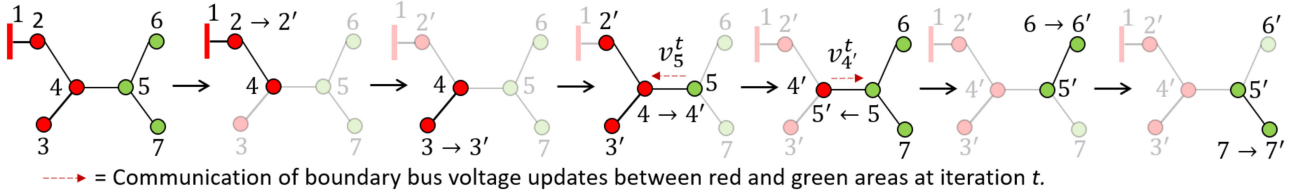
----> = Communication of boundary bus voltage updates between red and green areas at iteration *t*.

Fig. 2. A seven bus system with two areas (red & green) demonstrating the proposed distributed fixed point based algorithm.

Algorithm 1 Distributed FP algorithm for system with only PQ buses.

Input : P_i, Q_i for bus $i = 2, \cdots, n$ are specified values, Tolerance ζ for the stopping criterion.

Output: v_i for bus $i = 2, \cdots, n$.

1: Initialize voltages at all buses, v_i for $i = 2, \cdots, n$;
2: Let the neighboring bus index be k;
    where $k \in \mathcal{N}(m)$. $\triangleright \mathcal{N}(m)$: Neighboring buses of bus m.
3: Calculate power mismatch ($\Delta \mathbb{S} = \|p_i + q_i - (P_i + Q_i)\|_\infty$) $\forall i = 2, \cdots, n$; where p_i, q_i are calculated using (1a),(1b).
4: **while** ($\Delta \mathbb{S}) > \zeta$ **do** $\triangleright$ Convergence criteria.
5:    **for** $m = 2, \cdots, n$ **do**
6:      Calculate $(\mathbf{o}_p, r_p)$ at bus m, $\forall k \in \mathcal{N}(m)$;
7:      Calculate $(\mathbf{o}_q, r_q)$ at bus m, $\forall k \in \mathcal{N}(m)$;
8:      Calculate the voltage v_m for bus m using (18);
9:      $v_m = v_m$; $\triangleright$ Update current bus (m) voltage.
10:    **end for**
11:    Calculate ($\Delta \mathbb{S}$);
12: **end while**
13: **return** v_m $\forall$ buses $m = 2, \cdots, n$;

---

never observed the non-intersection of the circles. However for non-feasible problems, it is observed that the algorithm will have non-intersection of circles and further updates in the iterative process are not possible.

B. Basic Block in FP Method: Finding Intersection Points

In Algorithm 1, the main computation step is to find the intersection of two circles. At a first glance, this operation is almost trivial and there are many different ways to compute the intersections. However, the numerical implementation of an intersection algorithm can experience subtle but critical issues. First of all, this operation is called upon many times in the algorithm, and small errors can propagate and result in slower convergence speeds. Second of all, the circles can have very small or large radii. For example, if lines are close to being purely inductive (high X/R ratio), then the reactive circle becomes a circle with a very large radius and straightforward algorithms would run into numerical instabilities. Finally, since finding the intersections takes most of the time in Algorithm 1, it would be desirable to get as close to a closed-form solution as possible. Therefore, we use an unconventional representation of circles developed by [40] to provide a robust and efficient algorithm to find the intersection of circles. For ease of exposition, we focus

on system with PQ bus. Analogous results can be derived for PV buses.

Fig. 3 outlines the steps we take to derive the closed-form solution for the intersection of the active and reactive power circles. This is achieved in three steps. First, we find the line through the two circles (Fig. 3(a)). Then, we find the smallest circle (called the orthogonal circle) that passes through the intersecting points of the original circles (Fig. 3(b)). Next, we find the intersection of the line with the orthogonal circle (Fig. 3(c)) to obtain the proposed fixed-point equation. We present the derivation of fixed-point equation in the subsequent sections below by representing the circles in a vector space. It turns out that when we represent circles in a vector space, the above three step computations can be thought as vector manipulations, which is simple to perform and numerically stable. In the rest of this section, we develop this theory based on the material in [40].

C. For Numerical Stability: 3x1 Vector Presentation of Circles

Instead of the traditional center/radius parameterization, we can describe all of the points $\mathbf{x} \in \mathbb{R}^2$ on a circle by the following equation:

$$a(\mathbf{x} \cdot \mathbf{x}) + \mathbf{b} \cdot \mathbf{x} + c = 0, \tag{4}$$

where $\cdot$ denotes the dot product between two vectors. The form in (4) allows us to describe a circle using a three tuple $(a, \mathbf{b}, c)$. Note that this presentation is not unique, since scaling all of the parameters by a scalar does not change the points that satisfy (4). If a is not zero, we will scale parameters such that $a = 1$. In this notation, the circles described by the real and reactive power equations in (1a) and (1b) respectively becomes

$$(a_p, \mathbf{b}_p, c_p) = \left(1, \left[\frac{t_{d,2}}{t_{d,1}} \quad \frac{t_{d,3}}{t_{d,1}}\right]^T, -\frac{p_d}{t_{d,1}}\right), \tag{5}$$

and

$$(a_q, \mathbf{b}_q, c_q) = \left(1, \left[-\frac{t_{d,3}}{t_{d,4}} \quad \frac{t_{d,2}}{t_{d,4}}\right]^T, -\frac{q_d}{t_{d,4}}\right). \tag{6}$$

In these representations, the circles shift gracefully and the same calculations can be applied to a wide range of parameter values even if they approach zero or infinity.

Next, we separate the fixed parameters in the system (e.g., admittance values) and the voltages. Given a bus d, let $d_1, d_2, \ldots, d_k$ its neighboring nodes. Let $\mathbf{g}_d = \begin{bmatrix} g_{d_1,d} & g_{d_2,d} & \cdots & g_{d_k,d} \end{bmatrix}$ denote the vector of conductances between bus d and its neighbors. Similarly, let $\mathbf{b}_d = \begin{bmatrix} b_{d_1,d} & b_{d_2,d} & \cdots & b_{d_k,d} \end{bmatrix}$ denote the vector of susceptances.

(a) Equation of a line passing through common points of two circles.

(b) Orthogonal circle passing through common points of two circles.

(c) Point of intersection of orthogonal circle and the line passing through common points is $v_d = f(\mathbf{v})$.
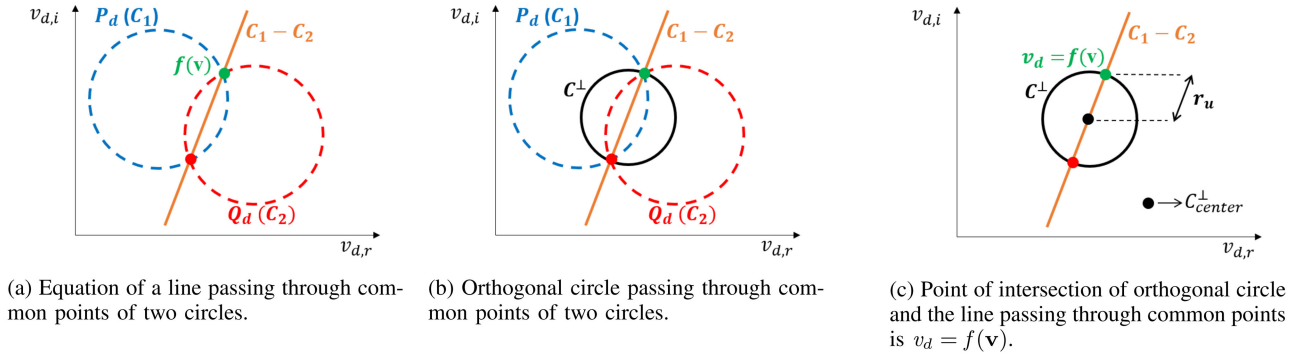
Fig. 3. Geometrical illustration of calculating the voltage solution at a bus. (a) Equation of a line passing through common points of two circles. (b) Orthogonal circle passing through common points of two circles. (c) Point of intersection of orthogonal circle and the line passing through common points is $vd = f(v)$.

Let $\mathbf{1}$ denote the vector of all 1's of the appropriate length. To represent the voltages of the neighboring buses, we use a vector $\mathbf{u}$ formed by concatenating the real and imaginary voltages:

$$\mathbf{u} = \begin{bmatrix} v_{d_1,r} & v_{d_2,r} & \cdots & v_{d_k,r} & v_{d_1,i} & v_{d_2,i} & \cdots & v_{d_k,i} \end{bmatrix}^T.$$

Then, we can rewrite (5) and (6) as

$$(a_p, \mathbf{b}_p, c_p) = \left(1, \begin{bmatrix} -\alpha & \delta \\ -\delta & -\alpha \end{bmatrix} \mathbf{u}, \frac{p_d}{\mathbf{1} \cdot \mathbf{g}_d} \right), \qquad (7)$$

$$(a_q, \mathbf{b}_q, c_q) = \left(1, \begin{bmatrix} -\beta & -\gamma \\ \gamma & -\beta \end{bmatrix} \mathbf{u}, \frac{-q_d}{\mathbf{1} \cdot \mathbf{b}_d} \right), \qquad (8)$$

where

$$\alpha = \frac{\mathbf{g}_d}{\mathbf{1} \cdot \mathbf{g}_d}, \beta = \frac{\mathbf{b}_d}{\mathbf{1} \cdot \mathbf{b}_d}, \gamma = \frac{\mathbf{g}_d}{\mathbf{1} \cdot \mathbf{b}_d}, \delta = \frac{\mathbf{b}_d}{\mathbf{1} \cdot \mathbf{g}_d}.$$

If needed, the centers and radii of power flow circles can be computed easily from (7) and (8):

$$\mathbf{o}_p = \frac{-\mathbf{b}_p}{2}, \mathbf{o}_q = \frac{-\mathbf{b}_q}{2}, \qquad (9)$$

$$r_p^2 = \left(\frac{\mathbf{b}_p \cdot \mathbf{b}_p}{4} - c_p\right), r_q^2 = \left(\frac{\mathbf{b}_q \cdot \mathbf{b}_q}{4} - c_q\right), \qquad (10)$$

where $\mathbf{o}_p$ and $\mathbf{o}_q$ are the centers of the real and reactive power circles, r_p and r_q are the radii, respectively.

D. Line Passing Through Intersection Points of the Power Flow Circles

Given two arbitrary circles $C_1 = (1, \mathbf{b}_1, c_1)$ and $C_2 = (1, \mathbf{b}_2, c_2)$, the line passing through their points of intersection is described by $C_1 - C_2$, provided the circles intersect. More formally, $C_1 - C_2$ is

$$C_1 - C_2 = (0, \mathbf{b}_1 - \mathbf{b}_2, c_1 - c_2) = (0, \mathbf{L}_2, L_3) \qquad (11)$$

and describes the points $\mathbf{v}_d$ that satisfies the equation

$$\mathbf{L}_2 \cdot \mathbf{v}_d + L_3 = 0, \qquad (12)$$

where

$$\mathbf{v}_d = \begin{bmatrix} v_{d,r} \\ v_{d,i} \end{bmatrix}.$$

Substituting (7) and (8) into (12), we have the line described by

$$\left(0, \begin{bmatrix} -\alpha+\beta & \gamma+\delta \\ -(\gamma+\delta) & -\alpha+\beta \end{bmatrix} \mathbf{u}, \frac{p_d}{\mathbf{1} \cdot \mathbf{g}_d} + \frac{q_d}{\mathbf{1} \cdot \mathbf{b}_d} \right). \qquad (13)$$

E. Orthogonal Circle

In principle, we can use the line computed in (13) to find the intersection points by intersecting that line with one of the active or reactive circles. However, the numerical accuracy and stability can suffer because the line may intersect the circles at a very acute angle. Therefore, it is more desirable to use the orthogonal circle for calculations. Geometrically, the orthogonal circle is the smallest circle that passes through the two intersection points. Algebraically, we label it as $C^\perp$. Again, the parameters of this circle can be computed from (7) and (8) via simple algebra [40], [41]:[1]

$$C^\perp = \left(a^\perp, \mathbf{b}^\perp, c^\perp\right)$$

$$= \left(1, \frac{\mathbf{b}_1 + \mathbf{b}_2}{2} + \frac{(\mathbf{b}_2 - \mathbf{b}_1)\left(k_1^2 - k_2^2\right)}{2\|\mathbf{b}_1 - \mathbf{b}_2\|^2}, \right.$$

$$\left. \frac{c_1 + c_2}{2} + \frac{(c_2 - c_1)\left(k_1^2 - k_2^2\right)}{2\|\mathbf{b}_1 - \mathbf{b}_2\|^2} \right), \qquad (14)$$

where

$$k_1^2 = \|\mathbf{b}_1\|^2 - 4a_1 c_1,$$

$$k_2^2 = \|\mathbf{b}_2\|^2 - 4a_2 c_2.$$

Here, $\| \ \|$ is the standard l_2 norm. The center and the radius of the orthogonal circle is given by

$$\mathbf{Center}^\perp = \frac{-\mathbf{b}^\perp}{2} \qquad (15)$$

[1] The original formula given in [40] is in fact incorrect and the right formula is given in [41].

and

$$r_u = \sqrt{\frac{\mathbf{b}^\perp \cdot \mathbf{b}^\perp}{4} - c^\perp}. \qquad (16)$$

Substituting (7) and (8) in (14), we get

$$C^\perp = \left(1, \frac{1}{2}\mathbf{M}_B\mathbf{u} + \frac{\left(\frac{\|\mathbf{u}\|^2}{2} \cdot K_c - 2 \cdot l\right)\mathbf{M}_A\mathbf{u}}{\|\mathbf{M}_A\mathbf{u}\|^2},\right.$$

$$\left.\frac{1}{2}\left(\frac{p_d}{\mathbf{1}\cdot\mathbf{g}_d} - \frac{q_d}{\mathbf{1}\cdot\mathbf{b}_d}\right) + \frac{l\left(2\,l - \frac{\|\mathbf{u}\|^2}{2}K_c\right)}{\|\mathbf{M}_A\mathbf{u}\|^2}\right), \quad (17)$$

where

$$\mathbf{M}_A = \begin{bmatrix} \boldsymbol{\alpha} - \boldsymbol{\beta} & -(\boldsymbol{\gamma} + \boldsymbol{\delta}) \\ \boldsymbol{\gamma} + \boldsymbol{\delta} & \boldsymbol{\alpha} - \boldsymbol{\beta} \end{bmatrix}$$

$$\mathbf{M}_B = \begin{bmatrix} -(\boldsymbol{\alpha} + \boldsymbol{\beta}) & \boldsymbol{\delta} - \boldsymbol{\gamma} \\ -(\boldsymbol{\delta} - \boldsymbol{\gamma}) & -(\boldsymbol{\alpha} + \boldsymbol{\beta}) \end{bmatrix},$$

$$l = \frac{p_d}{\mathbf{1}\cdot\mathbf{g}_d} + \frac{q_d}{\mathbf{1}\cdot\mathbf{b}_d},$$

$$K_c = \left(\|\boldsymbol{\alpha}\|^2 + \|\boldsymbol{\delta}\|^2\right) - \left(\|\boldsymbol{\gamma}\|^2 + \|\boldsymbol{\beta}\|^2\right).$$

F. Point of Intersection

Next, we find the point of intersection (Fig. 3(c)). These points are found at a distance of r_u from the center of orthogonal circle along the line computed in (13). Through simple algebra, we compute the point of intersection, that is, the updated voltage at bus d given by

$$\begin{bmatrix} v_{d,r} \\ v_{d,i} \end{bmatrix} = \mathbf{Center}^\perp \pm r_u \frac{\mathbf{RL}_2}{\|\mathbf{L}_2\|}$$

$$= -\frac{\mathbf{b}^\perp}{2} \pm \sqrt{\frac{\mathbf{b}^\perp \cdot \mathbf{b}^\perp}{4} - c^\perp} \cdot \frac{\mathbf{RL}_2}{\|\mathbf{L}_2\|},$$

$$= \frac{-1}{4}\mathbf{M}_B\mathbf{u} - \frac{\left(\frac{\|\mathbf{u}\|^2}{2}\cdot K_c - 2\cdot l\right)\mathbf{M}_A\mathbf{u}}{2\cdot\|\mathbf{M}_A\mathbf{u}\|^2} \pm$$

$$\left(\frac{1}{4}\cdot\left\|\frac{1}{2}\mathbf{M}_B\mathbf{u} + \frac{\left(\frac{\|\mathbf{u}\|^2}{2}\cdot K_c - 2\cdot l\right)\mathbf{M}_A\mathbf{u}}{\|\mathbf{M}_A\mathbf{u}\|^2}\right\|^2 -\right.$$

$$\frac{1}{2}\left(\frac{p_d}{\mathbf{1}\cdot\mathbf{g}_d} - \frac{q_d}{\mathbf{1}\cdot\mathbf{b}_d}\right) + \frac{l\left(2\,l - \frac{\|\mathbf{u}\|^2}{2}K_c\right)}{\|\mathbf{M}_A\mathbf{u}\|^2}\right)^{\frac{1}{2}}$$

$$\cdot\frac{\mathbf{RL}_2}{\|\mathbf{L}_2\|}. \qquad (18)$$

where

$$\mathbf{R} = \begin{bmatrix} 0 & -1 \\ 1 & 0 \end{bmatrix}$$

and $\mathbf{b}^\perp$ is given by (14) and $\mathbf{L}_2$ is given by (11). To choose one solution or a sign in (18), we will pick the one that leads to the higher voltage magnitude. Note that in (18), the terms $\mathbf{M}_A$, $\mathbf{M}_B$, and K_c has only network admittance parameters. Thus, these terms are required to be calculated only once at each bus in the network as they remain constant throughout the iterative process of the proposed power flow algorithm. Applying (18) to every bus d also gives us an analytical form of the fixed point equation for the complex voltages.

V. Numerical Results

In this section, simulation studies on standard IEEE test cases are presented, specifically $4, 14, 30, 33, 39, 57, 118, 2383$ and 3375 bus systems are used. Their information are obtained from the Matpower software. The proposed fixed point algorithm is compared with other power flow methods at nominal loading and heavy loading conditions. We also test the sensitivity of these algorithm to the initializaton points. In particular, we consider the following five algorithms: 1) **FP**, proposed algorithm; 2) **GS**, the standard Gauss-Seidel algorithm [42]; 3) **NR**, the standard Newton-Raphson algorithm; 4) **FDLF**, the fast decoupled load flow algorithm and 5) **Iwamoto**, a Jacobian-based adjustable step size method (sometimes called non-divergent or cubic interpolation power flow method) [18].

A. Performance of Proposed Method

First we study the convergence of the proposed FP algorithm on the standard 14-, 30- and 118-IEEE bus systems as shown in Fig. 4 under nominal loading conditions. As shown in Fig. 4, for these standard cases, the fixed point algorithm converges in tens of iterations. Since each iteration is cheap to compute, the convergence time is in 10 s of milliseconds.

Next, we compare the convergence speed of FP with NR and Iwamoto algorithms for a variety of systems. For this convergence speed study, instead of comparing different power flow methods at base case loading of different network sizes, it is better to compare different power flow methods at heavy loading scenarios because the number of iterations required to converge increases not only when the network size increases but also when a network is heavily loaded. Hence, we introduce a scaling parameter λ to scale the real powers of loads and generations,
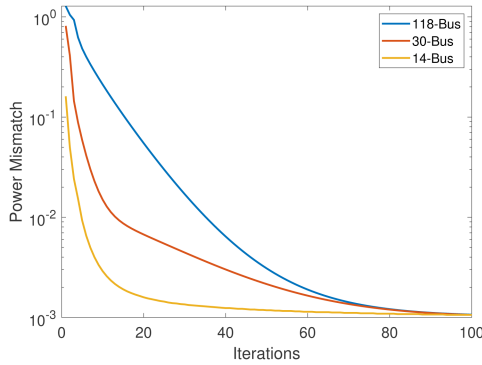
Fig. 4.   Semi-log plot of the convergence of the fixed point algorithm for IEEE standard systems at base case loading with bus switching.
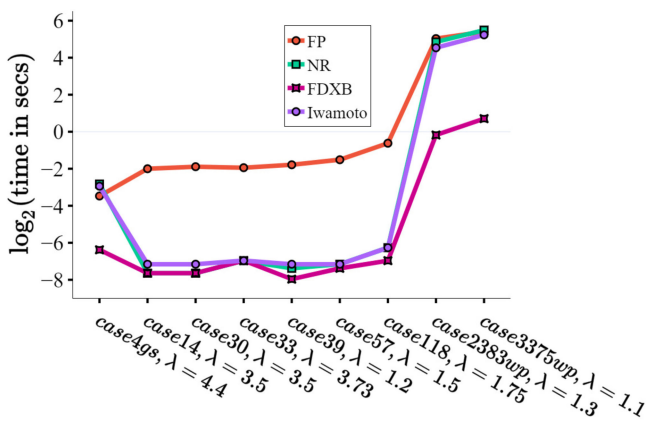

Fig. 5.   Time taken to attain the desired precision by FP, NR and Iwamoto's method for different size systems when load scaling parameter λ is maximum.
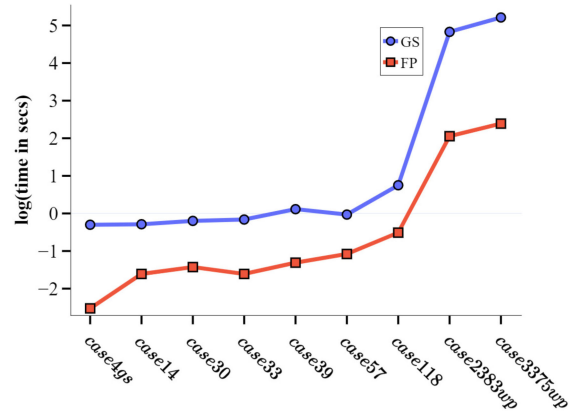

Fig. 6.   Time taken to attain the desired precision by GS and FP method for different size systems at base case loading.
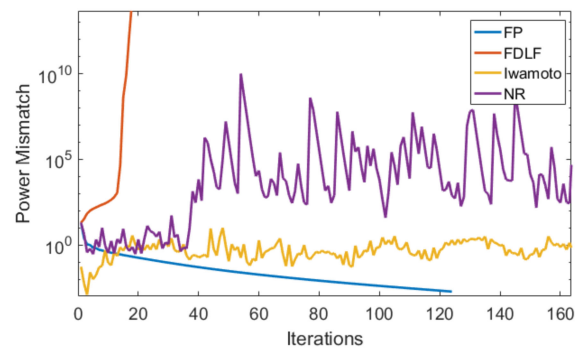

Fig. 7.   Convergence performance of FP compared with NR, Iwamoto and FDLF. The test system is the IEEE 14-bus system with loads scaled by a factor of 3.99.

and reactive powers of loads like [15], [43], [44]. For example, if the loads in the grid increase by only 1% then there is no need to re-dispatch as the slack bus can handle the load change. But if the total loading on the grid is increased by 200% and the generators are not re-dispatched (i.e., the P's in PV buses are not scaled) then the slack bus will have to handle a large load change. This may lead to the slack bus violating its Var limits and power ratings. Therefore the solution is more realistic if the setpoints of the PV buses are scaled together with the load.

Like [15], [18], [43], for each IEEE test system, the scaling factor λ is determined through a trial and error procedure. The goal is to increase λ until existing methods exhibit convergence issues. The time performance of all three algorithms are shown in Fig. 5 using a log-scale for different network sizes. The value of the scaling parameter λ for different networks in Fig. 5 shows the maximum power transfer capability of the corresponding network. None of the algorithms are tuned, in the sense that various parameter settings are at their default values. The proposed method is not faster than the existing methods and it is meant to serve as a complementary technique especially when existing algorithms diverge or stalls (presented in Section V-B). Fig. 6 compares the convergence speed of FP and GS for a variety of networks with different sizes. GS calculates the voltage solutions at every bus in the system via a lexicographical approach [42].

Even though GS is partly similar to the proposed approach, the fixed point equation used to calculate the voltages in both the methods are different. This difference makes the FP perform faster when compared to GS as shown in Fig. 6. From Fig. 5 and Fig. 6, it can be observed that the proposed method converges at heavy and base case loading conditions for both radial and mesh networks.

B. Heavily Loaded Networks

The more challenging setting for any power flow algorithm, and the setting the FP algorithm is designed to address, is when the systems are heavily loaded. For example, we take the 14-bus network and scale the loads and real power of the generators by a factor of 3.99. This loading is still feasible, but is very close to the loadability limit of the system. Fig. 7 presents the convergence comparison of the methods. The convergence criteria is that the infinity norm over the apparent power mismatch at all buses in the network must be less or equal to 0.001 p.u. on a 100 MVA base. From Fig. 7, the NR method given by the update equation $\mathbf{\Delta} V = (J^{-1}) \cdot (\mathbf{\Delta} S)$ diverges since the Jocabian matrix is very ill-conditioned around the solution. This is because when the power network is loaded to its maximum power transfer capability, the minimum singular
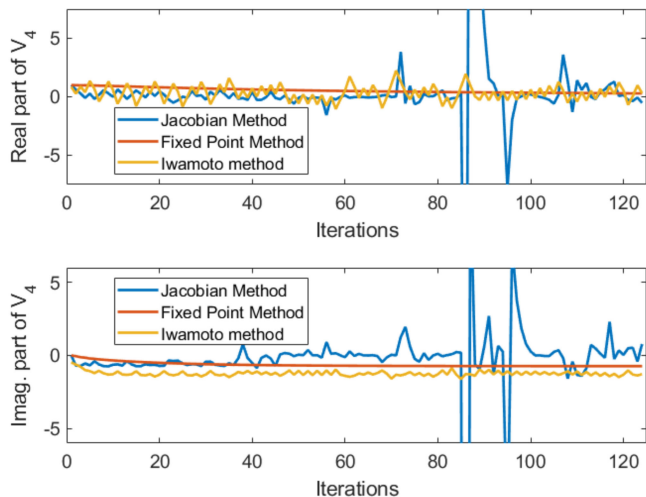
Fig. 8. Comparison of NR, FP and Iwamoto's voltage updates at bus 4 in IEEE-14 bus system under the loading condition of Fig. 7.

TABLE I
CONVERGENCE TEST OF THE POWER FLOW METHODS WITH RANDOM INITIALIZATION FOR 100 TRIALS. THE INITIAL VOLTAGES ARE GENERATED IDENTICAL AND INDEPENDENTLY FROM UNIFORM DISTRIBUTION OF $[1 - \chi, 1 + \chi]$

Initialization spread χ	NR	FDLF	Iwamoto	FP
0.05	100	98	100	100
0.1	64	62	100	100
0.3	0	0	0	100
0.4	0	0	0	100

value of the J becomes very close to zero and it results in a close to infinite condition number of the matrix J due to finite machine precision [45]. Thus, as shown in Fig. 7, NR method diverges. [45] shows that for bigger network sizes, the faster NR method diverges while the matrix-free methods do not have error in convergence accuracy. A variety of robust variations of the basic Newton's method were proposed to solve this problem. One such technique is Iwamoto's method [18]. Majority of these new techniques modify $\Delta V = (J^{-1}) \cdot (\Delta S)$ to include the multiplier μ to control the step size for the updates i.e., $\Delta V = \mu \cdot (J^{-1}) \cdot (\Delta S)$. However, if J is very close to being singular then J^{-1} cannot be accurately calculated due to limited machine precision [18], [45]. Hence, from Fig. 7, the Iwamoto's method [18] also becomes unstable because of numerical issues. The FDLF also diverges, while it does not face conditioning problems since the Jacobian is approximated by a fixed matrix in decoupled load flow, the update direction provided by the fixed Jacobian becomes invalid and the algorithm diverges very quickly. Thus, as shown in Fig. 7, we not only provide a matrix free iterative method to avoid the pitfalls of high condition number of the Jacobian but we also provide a fixed-point method which is much faster and stable than the GS method as highlighted in [45]. Alternatively, the proposed method can also be used to obtain better initial voltage estimates for NR based method in case of a hard-to-solve scenario. Similar behaviors to Fig. 7 are observed in IEEE 4-, 30- and 118-bus systems for load multiplier of 4.5, 3.65 and 1.78, respectively. In contrast, our proposed method is able to converge even under these conditions since it does not use the power flow Jacobian. This illustrates the envisioned utility of the proposed FP method in practice. An operator can use conventional power flow solvers and when they do not converge, instead of fine tuning parameters or trying many different initialization points, the FP algorithm can be used as a viable tool to obtain convergence.

Figure 8 compares the performance of the FP, NR, and Iwamoto algorithms in more detail. As we can see, the NR

algorithm jumps erratically in the voltage space. The Iwamoto method controls this behavior by scaling the updates by μ, but even though it prevents the algorithm from diverging, it cannot converge reliably and instead oscillate around the solution. The FP algorithm again converges reliably and do not oscillate. Thus, FP algorithm has the highest convergence accuracy since it does not encounter the numerical instabilities like NR, Iwamoto, and FDLF since the only calculation required is the intersection of two circles (regardless of the network size), and these intersections can be handled gracefully using the proposed matrix free algorithm. We also observed the proposed FP method is more stable than the GS method but it is omitted from the results due to interest of space in the paper during first draft.

C. Sensitivity to Initial Conditions

In addition to convergence, it is important for an algorithm to be robust to the initial conditions, especially as the uncertainty in the system increases due to renewable integration . To test the performance of various algorithms to initial conditions, we take the IEEE 30-bus system at its standard loading and randomly select the starting voltages. In our experiments, we set the initial guess to be random samples from the uniform distribution on the interval $[1 - \chi, 1 + \chi]$ for various values of χ (we always set the imaginary part to be 0), independently for each bus. Table I reports the number of successful convergences (defined as power mismatch convergence less than 0.001 p.u.) for the FDLF, NR, Iwamoto and our proposed FP methods for 100 trials.

As we see in Table I, our proposed FP method is much more robust to the value of the initial guesses than the other methods: it always converged while the other methods quickly stopped working when α becomes large. Hence it is observed that the phenomenon of power flow fractals is not exhibited by the proposed method unlike NR based methods. This hints that the fixed point method may avoid being trapped in local optima that can impact descent algorithms since local optima are not fixed points by definition.

D. Distributed Approximation-Free Multi-Area Power System Analysis

Network equivalence and mathematical decomposition techniques are widely used to solve for multi-area AC power flow in a distributed or decentralized manner [37], [46], [47]. By distributed, we mean that areas connected by tie lines do not need

(a) IEEE 118-bus system.
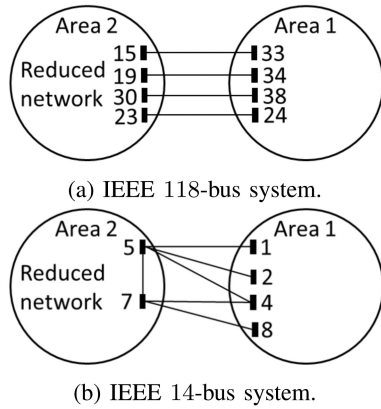

(b) IEEE 14-bus system.

Fig. 9. Power networks with two areas.

TABLE II
TOTAL NUMBER OF LINES WHOSE BRANCH FLOW (APPARENT POWER) ERROR IS GREATER THAN THE DESIRED THRESHOLD OF 0.01 P.U. OR 1 MVA IN CASE OF REI AND PROPOSED METHOD FOR IEEE 14 AND 118-BUS SYSTEMS

IEEE power network	Total branches in area 1	REI method - Total lines where $S^{error} > 1$ MVA	Proposed method - Total lines where $S^{error} > 1$ MVA
4-bus grid	9	3	0
118-bus grid	144	16	0

to share their internal information with each other. We selected a standard network equivalence technique known as REI method as it is widely used in the literature of multi-area power system analysis [48]–[55]. Also, when a distributed algorithm is based on matrix-based formulations like NR or FDLF, if the centralized versions do not converge, then the distributed version do not either.

Let us consider the IEEE 14 and 118-bus systems with two areas as shown in Fig. 9(b) and Fig. 9(a). The boundary buses are represented in these two areas. The buses other than boundary buses in area 2 are eliminated and represented by the equivalent network. Among these eliminated nodes, all PQ buses are represented by one REI network equivalent/node, and all PV buses are represented by a separate REI network equivalent/node for accurate modeling [50], [52]. The purpose is to solve the area 1 power flow problem without requiring the area 2 information which is represented by two REI equivalent nodes (one node representing all PQ buses in area 2 and the other node representing all PV buses in area 2).

The solution quality is evaluated based on branch flows in area 1 since the error in voltage phasor solution will be reflected in branch flows [46], [52], [53]. The flow error of a branch ($S_{d,k}^{error}$) connecting buses d, and k is defined as the difference between actual branch flow and the calculated branch flow using either the REI or proposed method.

Table II presents the total number of branches in which the branch flow error (S^{error}) is greater than the tolerance of 0.01 p.u. (1 MVA). It can be observed that the REI method has a total of 3 (out of 9) and 16 (out of 144) branches in area 1 of IEEE 14, and 118-bus systems respectively whose flow error violates
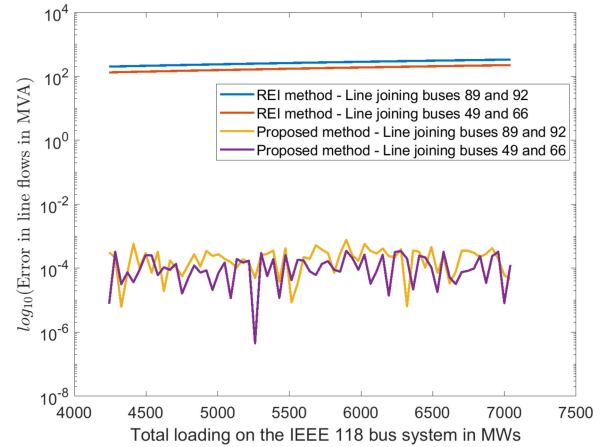
(a) Error in branch flows for both REI and proposed method at different operating conditions in base 10-logarithmic scale for IEEE 118-bus system shown in Fig. 9a.
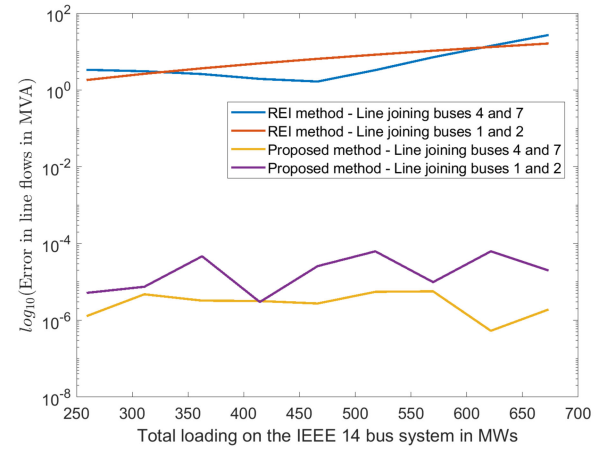
(b) Error in branch flows for both REI and proposed method at different operating conditions in base 10-logarithmic scale for IEEE 14-bus system shown in Fig. 9b.

Fig. 10. Comparison of branch flow errors between the REI and proposed method for different operating conditions on IEEE 118 and 14-bus systems. (a) Error in branch flows for both REI and proposed method at different operating conditions in base 10-logarithmic scale for IEEE 118-bus system shown in Fig. 9a. (b) Error in branch flows for both REI and proposed method at different operating conditions in base 10-logarithmic scale for IEEE 14-bus system shown in Fig. 9b.

the tolerance of 0.01 p.u. Whereas the proposed method has 0 branches whose flow error violates the set tolerance. In addition, the flow error values of all branches in area 1 using the proposed method are observed to be very close to 0 MVA.

In addition, Fig. 10(a) shows the branch flow errors (log scaled MVA) of 2 branches from area 1 of the IEEE 118-bus system for various operating conditions in the case of both REI and proposed method. Similarly, Fig. 10(b) shows the branch flow errors of 2 branches from area 1 of the IEEE 14-bus system. It can be observed that the error in branch flows is negligible in the case of the proposed method while it is not negligible for the REI method for various operating conditions. A similar observation can also be made for Fig. 10(b). This error in the REI method is mainly due to approximation error caused by

the linearized representation of the non-linear power grid loads. Because of this reason, it is hard to obtain a good REI equivalent network of area 2 that works well on different operating conditions. However, the approximation-free nature of the proposed method with negligible branch flow errors showcases the applicability of the proposed method in multi-area power system analysis.

VI. CONCLUSION

A new fixed-point formulation of the power flow equation is developed in this paper. The distributed feature of the proposed ACPF enables to develop distributed AC OPFs that does not require the private information exchange between two different entities. In contrast to existing distributed methods for multi-area power system analysis, the proposed distributed method does not use any approximate equivalents of other areas and is more accurate. In contrast to existing fixed point formulations, it includes all possible cases of PV/PQ buses, mesh networks, resistive and inductive lines. Geometrically, our formulation treats the active and reactive power flow equations as circles and the power flow solutions as the intersection of these circles. Using a 3-tuple vector representation of circles, we derive simple, efficient and numerically stable equation. Numerical studies on the standard IEEE benchmarks show that our algorithm is able to converge when other state-of-the-art robust algorithms diverges. We also show that the performance of proposed algorithm is comparable to other Jacobian based methods for large test systems. In addition, we show that our algorithm is robust to the initial starting point, able to converge for a wide range of starting conditions while other algorithms diverged.

APPENDIX

A. Handling PQ and PV Buses

Here we present the fixed-point algorithm for a system with both PQ and PV buses. In the case of PV buses, Section II-B discusses the replacement of the reactive power balance equation by a condition on the voltage magnitude (3). The voltage circle is centered at origin ($\mathbf{o}_v$) with fixed radius of V_{ref} (r_v). Thus the voltage solution for a PV bus can be calculated similarly to PQ bus by the intersection of two circles, real power (1a) and specified voltage magnitude circles (3) at bus d.

B. Bus Type Switching for PV Buses

1) PV to PQ Switching: When there are no common points between the real power and specified voltage magnitude circles, the reactive power at bus d is calculated to check for the violation of reactive power limits. In such a scenario, the PV bus is converted to a PQ bus by fixing its reactive power with the violated limit and it is then solved as a PQ bus. During the iterative process, this PQ bus is converted back to a PV bus as discussed below.

2) PQ to PV Switching: The bus that is converted to PQ has its real and reactive power fixed while the voltage phase angle and magnitude are free to change. However, this bus should be reverted to PV bus during the power flow iterative process

---

Algorithm 2 FP method for PQ and PV buses.

> **Input :** P_i for bus $i = 2, \cdots, n$,
> $\qquad\quad Q_i \;\forall$ PQ buses,
> $\qquad\quad V_{ref} \;\forall$ PV buses,
> $\qquad\quad Q_{max}$ and Q_{min} for PV buses,
> $\qquad\quad$ Bus type information $\mathbf{B}\{i\}$ for bus $i = 2, \cdots, n$,
> $\qquad\quad$ Tolerance ζ for the stopping criterion.
> **Output:** v_i for bus $i = 2, \cdots, n$.

1: Initialize voltages at all buses, v_i for $i = 2, \cdots, n$;
2: Let the neighboring bus index be k;
$\quad$ where $k \in \mathcal{N}(m)$. $\qquad \triangleright \mathcal{N}(m)$: Neighboring buses to m.
3: Calculate power mismatch ($\Delta\mathbb{S} = \|p_i + q_i - (P_i + Q_i)\|_\infty$) $\forall\, i = 2, \cdots, n$; where p_i, q_i are calculated using (1a),(1b) and reactive power mismatch $q_i - Q_i = 0 \;\forall\; i \in$ PV buses.
4: **while** $(\Delta\mathbb{S}) > \zeta$ **do** $\qquad\qquad \triangleright$ Convergence criteria.
5: $\quad$ **for** $m = 2, \cdots, n$ **do**
6: $\quad\quad$ **if** $\mathbf{B}\{m\} ==$ PQ bus **then**
7: $\quad\quad\quad$ Calculate $(\mathbf{o}_p, r_p)$ at bus m, $\forall\; k \in \mathbb{N}_m$;
8: $\quad\quad\quad$ Calculate $(\mathbf{o}_q, r_q)$ at bus m, $\forall\; k \in \mathbb{N}_m$;
9: $\quad\quad\quad$ Calculate the voltage v_m for bus m using (18);
10: $\quad\quad\quad v_m = v_m$; $\qquad\qquad \triangleright$ Update bus m voltage.
11: $\quad\quad\quad$ **if** $\mathbf{B}\{m\} == PQ_{max}$ and $v_m > V_{ref}$ **then**
12: $\quad\quad\quad\quad$ Revert to PV bus and update $B\{m\}$;
13: $\quad\quad\quad$ **end if**
14: $\quad\quad\quad$ **if** $\mathbf{B}\{m\} == PQ_{min}$ and $v_m < V_{ref}$ **then**
15: $\quad\quad\quad\quad$ Revert to PV bus and update $B\{m\}$;
16: $\quad\quad\quad$ **end if**
17: $\quad\quad$ **else** $\qquad\qquad\qquad\qquad\qquad \triangleright$ PV bus.
18: $\quad\quad\quad$ Calculate $(\mathbf{o}_p, r_p)$ at bus m, $\forall\; k \in \mathbb{N}_m$;
19: $\quad\quad\quad$ Calculate $(\mathbf{o}_v, r_v)$ at bus m, $\forall\; k \in \mathbb{N}_m$;
20: $\quad\quad\quad$ **if** Circles $(\mathbf{o}_p, r_p)$ and $(\mathbf{o}_v, r_v)$ intersect **then**
21: $\quad\quad\quad\quad$ Calculate the voltage v_m for bus m (18);
22: $\quad\quad\quad\quad \angle v_m = \angle v_m$; $\qquad \triangleright$ Update voltage angle.
23: $\quad\quad\quad$ **else**
24: $\quad\quad\quad\quad$ Convert bus m to PQ bus & update $\mathbf{B}\{m\}$;
25: $\quad\quad\quad\quad$ Calculate $(\mathbf{o}_p, r_p)$ at bus m;
26: $\quad\quad\quad\quad$ Calculate $(\mathbf{o}_q, r_q)$ at bus m;
27: $\quad\quad\quad\quad$ Calculate the voltage v_m for bus m (18);
28: $\quad\quad\quad\quad v_m = v_m$; $\qquad \triangleright$ Update bus m voltage.
29: $\quad\quad\quad$ **end if**
30: $\quad\quad$ **end if**
31: $\quad$ **end for**
32: $\quad$ Calculate $(\Delta\mathbb{S})$;
33: **end while**
34: **return** $v_m \;\forall$ buses $m = 2, \cdots, n$;

---

when it is feasible since the problem still didn't converge. Let the voltage solution at this converted PQ bus be v. The violated upper and lower limit reactive powers be represented by Q_{max} and Q_{min} respectively. A converted PQ bus (due to PV to PQ switching) with $Q = Q_{max}$ or $Q = Q_{min}$ is referred as PQ_{max} bus or PQ_{min} bus respectively. For PQ_{max} bus, when $v > V_{ref}$ it indicates that the reactive power at this bus is no longer needed to be fixed at Q_{max} and it can be reverted back to a PV bus. Similarly for PQ_{min} bus when $v < V_{ref}$, it is no longer needed for the reactive power to be fixed at Q_{min} and PQ_{min} bus can be reverted back to a PV bus.
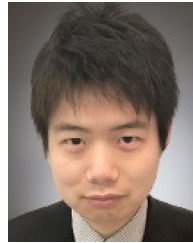
REFERENCES

[1] B. Stott, "Review of load-flow calculation methods," *Proc. IEEE>*, vol. 62, no. 7, pp. 916–929, Jul. 1974.

[2] J. A. Momoh, M. E. El-Hawary, and R. Adapa, "A review of selected optimal power flow literature to 1993. II. Newton, linear programming and interior point methods," *IEEE Trans. Power Syst.*, vol. 14, no. 1, pp. 105–111, Feb. 1999.

[3] B. Stott and O. Alsac, "Fast decoupled load flow," *IEEE Trans. Power App. Syst.*, vol. PAS-93, no. 3, pp. 859–869, May 1974.

[4] A. Monticelli, A. Garcia, and O. R. Saavedra, "Fast decoupled load flow: Hypothesis, derivations, testing," *IEEE Trans. Power Syst.*, vol. 5, no. 4, pp. 1425–1431, Nov. 1990.

[5] PEW Trusts, "Electric cars will challenge state power grids," 2020. [Online]. Available: https://www.pewtrusts.org/en/research-and-analysis/blogs/stateline/2020/01/09/electric-cars-will-challenge-state-power-grids

[6] M. Power, "Driving change on the grid - The impact of EV adoption," 2020. [Online]. Available: https://www.powermag.com/driving-change-on-the-grid-the-impact-of-ev-adoption

[7] Charge Point Inc., "Electric vehicle growth projections and market share," 2019. [Online]. Available: https://www.chargepoint.com/about/news/chargepoint-releases-list-top-10-regions-electric-vehicle-growth/

[8] J. Thorp and S. Naqvi, "Load flow fractals," in *Proc. 28th IEEE Conf. Decis. Control*, 1989, pp. 1822–1827.

[9] D. Pudjianto, C. Ramsay, and G. Strbac, "Virtual power plant and system integration of DERs," *IET Renewable Power Gener.*, vol. 1, no. 1, pp. 10–16, 2007.

[10] B. Zhang and D. Tse, "Geometry of injection regions of power networks," *IEEE Trans. Power Syst.*, vol. 28, no. 2, pp. 788–797, May 2013.

[11] I. A. Hiskens and R. J. Davy, "Exploring the power flow solution space boundary," *IEEE Trans. Power Syst.*, vol. 16, no. 3, pp. 389–395, Aug. 2001.

[12] V. Ajjarapu and C. Christy, "The continuation power flow: A tool for steady state voltage stability analysis," *IEEE Trans. Power Syst.*, vol. 7, no. 1, pp. 416–423, Feb. 1992.

[13] B. Stott, "Effective starting process for Newton-Raphson load flows," *Proc. Inst. Elect. Engineers*, vol. 118, no. 8, pp. 983–987, 1971.

[14] H.-D. Chiang, T.-Q. Zhao, J.-J. Deng, and K. Koyanagi, "Homotopy-enhanced power flow methods for general distribution networks with distributed generators," *IEEE Trans. Power Syst.*, vol. 29, no. 1, pp. 93–100, Jan. 2014.

[15] A. Gómez-Expósito and C. Gómez-Quiles, "Factorized load flow," *IEEE Trans. Power Syst.*, vol. 28, no. 4, 4607–4614, Nov. 2013.

[16] W. F. Tinney and C. E. Hart, "Power flow solution by newton's method," *IEEE Trans. Power App. Syst.*, vol. PAS-86, no. 11, pp. 1449–1460, Nov. 1967.

[17] A. Shahriari, H. Mokhlis, and A. Bakar, "Critical reviews of load flow methods for well, ill and unsolvable condition," *J. Elect. Eng.*, vol. 63, no. 3, pp. 144–152, 2012.

[18] S. Iwamoto and Y. Tamura, "A load flow calculation method for ill-conditioned power systems," *IEEE Trans. Power App. Syst.*, vol. PAS-100, no. 4, pp. 1736–1743, Apr. 1981.

[19] C. Castro and L. Braz, "A new approach to the polar newton power flow using step size optimization," in *Proc. 29th North Amer. Symp.*, Laramie, Wyoming, USA, 1997, pp. 121–133.

[20] L. M. Braz, C. A. Castro, and C. Murati, "A critical evaluation of step size optimization based load flow methods," *IEEE Trans. Power Syst.*, vol. 15, no. 1, pp. 202–207, Feb. 2000.

[21] P. R. Bijwe and S. M. Kelapure, "Nondivergent fast power flow methods," *IEEE Trans. Power Syst.*, vol. 18, no. 2, pp. 633–638, May 2003.

[22] M. Pirnia, C. A. Cañizares, and K. Bhattacharya, "Revisiting the power flow problem based on a mixed complementarity formulation approach," *IET Gener., Transmiss. Distrib.*, vol. 7, no. 11, pp. 1194–1201, 2013.

[23] Y.-H. Moon, H.-J. Koo, J.-G. Lee, Y.-J. Kwon, and B.-M. Yang, "Energy-based power system analysis with the equivalent mechanical model," *IFAC Proc. Volumes*, vol. 36, no. 20, pp. 599–604, 2003.

[24] S. Li, D. Tylavsky, D. Shi, and Z. Wang, "Implications of Stahl's theorems to holomorphic embedding Pt. I: Theoretical convergence," *CSEE J. Power Energy Syst.*, vol. 7, no. 4, pp. 761–772, Jul. 2021, doi: 10.17775/CSEE-JPES.2020.01910.

[25] A. Dronamraju *et al.*, "Implications of Stahl's theorems to holomorphic embedding Pt. II: Numerical convergence," *CSEE J. Power Energy Syst.*, vol. 7, no. 4, pp. 773–784, Jul. 2021, doi: 10.17775/CSEE-JPES.2020.01920.

[26] A. G. Bakirtzis, P. N. Biskas, C. E. Zoumas, and V. Petridis, "Optimal power flow by enhanced genetic algorithm," *IEEE Trans. power Syst.*, vol. 17, no. 2, pp. 229–236, May 2002.

[27] M. A. Abido, "Optimal power flow using particle swarm optimization," *Int. J. Elect. Power Energy Syst.*, vol. 24, no. 7, pp. 563–571, 2002.

[28] H. Oh, "A unified and efficient approach to power flow analysis," *Energies*, vol. 12, no. 12, 2019, Art. no. 2425.

[29] J. W. Simpson-Porco, "A theory of solvability for lossless power flow equations-Part I: Fixed-point power flow," *IEEE Trans. Control Netw. Syst.*, vol. 5, no. 3, pp. 1361–1372, Sep. 2017.

[30] C. Wang, A. Bernstein, J.-Y. Le Boudec, and M. Paolone, "Explicit conditions on existence and uniqueness of load-flow solutions in distribution networks," *IEEE Trans. Smart Grid*, vol. 9, no. 2, pp. 953–962, Mar. 2016.

[31] S. Kakutani *et al.*, "A generalization of Brouwer's fixed point theorem," *Duke Math. J.*, vol. 8, no. 3, pp. 457–459, Mar. 1941.

[32] A. Bernstein, C. Wang, E. Dall'Anese, J.-Y. Le Boudec, and C. Zhao, "Load flow in multiphase distribution networks: Existence, uniqueness, non-singularity and linear models," *IEEE Trans. Power Syst.*, vol. 33, no. 6, pp. 5832–5843, Nov. 2018.

[33] S. Y. Bocanegra, W. Gil-González, and O. D. Montoya, "A new iterative power flow method for AC distribution grids with radial and mesh topologies," in *IEEE Int. Autumn Meeting Power, Electron. Comput.*, 2020, pp. 1–5.

[34] L. F. Grisales-Noreña, O. D. Montoya, W. J. Gil-González, A.-J. Perea-Moreno, and M.-A. Perea-Moreno, "A comparative study on power flow methods for direct-current networks considering processing time and numerical convergence errors," *Electronics*, vol. 9, no. 12, 2020, Art. no. 2062.

[35] Y. Phulpin, M. Begovic, M. Petit, J.-B. Heyberger, and D. Ernst, "Evaluation of network equivalents for voltage optimization in multi-area power systems," *IEEE Trans. Power Syst.*, vol. 24, no. 2, pp. 729–743, May 2009.

[36] Z. Haibo, Z. Boming, S. Hongbin, and A. Ran, "A new distributed power flow algorithm between multi-control-centers based on asynchronous iteration," in *IEEE Int. Conf. Power Syst. Technol.*, 2006, pp. 1–7.

[37] M. G. Echeverri, J. M. L. Lezama, and J. R. S. Mantovani, "Decentralized AC power flow for multi-area power systems using a decomposition approach based on lagrangian relaxation," *Revista Facultad de Ingeniería Universidad de Antioquia*, vol. 23, pp. 225–235, 2010.

[38] B. K. Johnson, "Extraneous and false load flow solutions," *IEEE Trans. Power App. Syst.*, vol. 96, no. 2, pp. 524–534, Mar. 1977.

[39] P. Kundur, N. J. Balu, and M. G. Lauby, *Power System Stability and Control*. New York, NY, USA: McGraw-Hill, 1994, pp. 20–22.

[40] A. E. Middleditch, T. Stacey, and S. B. Tor, "Intersection algorithms for lines and circles," *ACM Trans. Graph.*, vol. 8, no. 1, pp. 25–40, 1988.

[41] H. G. Baker, "Corrigenda: Intersection algorithms for lines and circles," *ACM Trans. Graph.*, vol. 13, no. 3, pp. 308–310, 1994.

[42] A. Keyhani, A. Abur, and S. Hao, "Evaluation of power flow techniques for personal computers," *IEEE Trans. Power Syst.*, vol. 4, no. 2, pp. 817–826, May 1989.

[43] Y.-S. Zhang and H.-D. Chiang, "Fast Newton-FGMRES solver for large-scale power flow study," *IEEE Trans. Power Syst.*, vol. 25, no. 2, pp. 769–776, May 2010.

[44] J.-J. Deng, T.-Q. Zhao, H.-D. Chiang, Y. Tang, and Y. Wang, "Convergence regions of Newton method in power flow studies: Numerical studies," in *Proc. IEEE Int. Symp. Circuits Syst.*, 2013, pp. 1532–1535.

[45] A. Pyzara, B. Bylina, and J. Bylina, "The influence of a matrix condition number on iterative methods' convergence," in *Proc. Federated Conf. Comput. Sci. Inf. Syst.*, 2011, pp. 459–464.

[46] L. Min and A. Abur, "Total transfer capability computation for multi-area power systems," *IEEE Trans. Power Syst.*, vol. 21, no. 3, pp. 1141–1147, Aug. 2006.

[47] L. Min and A. Abur, "Decomposition algorithms for multi-area power system analysis," Ph.D. dissertation, Texas A&M University, 2007.

[48] P. Dimo, *Nodal Analysis of Power Systems*. Bucureşti: Editura Academiei Republicii Socialisté România, 1975, pp. 35–48. [Online]. Available: https://www.worldcat.org/title/nodal-analysis-of-power-systems/oclc/2118737

[49] W. Tinney and W. Powell, "The REI approach to power network equivalents," *IEEE Proc. PICA Conf.*, vol. 314, pp. 314–320, May 1977.

[50] F. F. Wu and A. Monticelli, "Critical review of external network modelling for online security analysis," *Int. J. Elect. Power Energy Syst.*, vol. 5, no. 4, pp. 222–235, 1983.

[51] S. Deckmann, A. Pizzolante, A. Monticelli, B. Stott, and O. Alsac, "Studies on power system load flow equivalencing," *IEEE Trans. Power App. Syst.*, vol. PAS-99, no. 6, pp. 2301–2310, Nov. 1980.

[52] E. Housos, G. Irisarri, R. Porter, and A. Sasson, "Steady state network equivalents for power system planning applications," *IEEE Trans. Power App. Syst.*, vol. PAS-99, no. 6, pp. 2113–2120, Nov. 1980.

[53] T. D. Liacco, S. Savulescu, and K. Ramarao, "An on-line topological equivalent of a power system," *IEEE Trans. Power App. Syst.*, vol. PAS-97, no. 5, pp. 1550–1563, Sep. 1978.

[54] J. Stadler and H. Renner, "Application of dynamic REI reduction," in *IEEE PES Innov. Smart Grid Technol.*, 2013, pp. 1–5, doi: 10.1109/ISG-TEurope.2013.6695311.

[55] A. P. Gupta, A. Mohapatra, and S. Singh, "Power system network equivalents: Key issues and challenges," in *IEEE TENCON Region 10 Conf.*, 2018, pp. 2291–2296.

Yang Weng (Senior Member, IEEE) received the M.Sc. degree in machine learning of computer science and the M.E. and Ph.D. degrees in electrical and computer engineering from Carnegie Mellon University (CMU), Pittsburgh, PA, USA. After Ph.D., he joined Stanford University, Stanford, CA, USA, as the TomKat Fellow for Sustainable Energy. He is currently an Assistant Professor of electrical, computer and energy engineering with Arizona State University (ASU), Tempe, AZ, USA. His research interest focuses on machine learning for power systems.

Dr. Weng was the recipient of the CMU Dean's Graduate Fellowship in 2010, the Best Paper Award at the International Conference on Smart Grid Communication (SGC) in 2012, the first ranking paper of SGC in 2013, Best Papers at the Power and Energy Society General Meeting in 2014, ABB fellowship in 2014, Golden Best Paper Award at the International Conference on Probabilistic Methods Applied to Power Systems in 2016, and Best Paper Award at IEEE Conference on Energy Internet and Energy system Integration in 2017, Best Paper Award at the IEEE North American Power Symposium in 2019, and Best Paper Award at the IEEE Sustainable Power and Energy Conference in 2019.

Kishan Prudhvi Guddanti (Student Member, IEEE) received the B.Tech. degree in electrical engineering from the Sri Ramaswamy Memorial Institute of Science and Technology, Chennai, India, and the M.Sc. degree in electrical engineering from Arizona State University, Tempe, AZ, USA. He is currently working toward the Ph.D. degree with Arizona State University, Tempe, AZ, USA. His team is one of the winning teams of L2RPN AI competition organized by RTE France in 2019. He received Engineering Graduate Fellowship, and Graduate & Professional Student Scholarship in 2019. His current research interests include the interdisciplinary area of AI applications in power systems in addition to voltage stability, and data-driven techniques for power system risk assessment and control.

Baosen Zhang (Member, IEEE) received the Bachelor of Applied Science degree in engineering science from the University of Toronto, Canada, in 2008, and the Ph.D. degree in electrical engineering and computer sciences from the University of California, Berkeley, in 2013. He was a Postdoctoral Scholar with Stanford University.

He is currently an Assistant Professor in electrical and computer engineering with the University of Washington, Seattle, WA. His research interests include control, optimization and learning applied to power systems and other cyberphysical systems. He was the recipient of the NSF CAREER Award as well as several Best Paper Awards.